Degenerate four-wave mixing mediated by ponderomotive-force-driven plasma gratings

K.-H. Lee,[1] C.-H. Pai,[1,2] M.-W. Lin,[1] L.-C. Ha,[1,2] J.-Y. Lin,[3] J. Wang,[1,2,4] and S.-Y. Chen[1,4]
[1]*Institute of Atomic and Molecular Sciences, Academia Sinica, Taipei 106, Taiwan*
[2]*Department of Physics, National Taiwan University, Taipei 106, Taiwan*
[3]*Department of Physics, National Chung Cheng University, Chia-Yi 621, Taiwan*
[4]*Department of Physics, National Central University, Jhongli 320, Taiwan*
(Received 12 November 2006; published 26 March 2007)

Degenerate four-wave mixing mediated by ponderomotive-force-driven plasma gratings is demonstrated in the near-infrared regime. The quadratic dependence of the reflectivity of the probe pulse on plasma density indicates that the mixing is caused by the quasineutral plasma grating driven by the laser ponderomotive force. The experiment verifies that ponderomotive force is an effective means to produce a large-amplitude short-period plasma grating, which has many important applications in ultrahigh-intensity optics. In particular, such a grating is a crucial element for the development of plasma phase-conjugate mirrors that can be used to restore the wave-front distortion that is ubiquitous in nonlinear propagation.

DOI: 10.1103/PhysRevE.75.036403 PACS number(s): 52.35.Mw, 42.65.Hw, 52.50.Jm

I. INTRODUCTION

Development of the chirped-pulse amplification technique [1] has raised the peak power of ultrashort pulse lasers by several orders of magnitude. With this technique, the limiting factor on the peak power has been shifted from the nonlinear effects in the amplifier to the optical damage threshold of the pulse compressor. To overcome this limitation in future development, it was suggested that superradiant amplification or Raman back amplification in plasma can be used to amplify and compress the laser pulses [2,3]. Such schemes are not prone to optical damage. However, at the laser intensity targeted by these schemes, thermal effects and nonlinear effects may cause severe wave-front distortion. Therefore even without permanent damage, one still faces the challenge of wave-form instability. It is well established that phase-conjugate mirrors (PCMs) based on degenerate four-wave mixing (DFWM) can be used to compensate for wave-front distortion [4–6]. In DFWM, two counterpropagating pump beams and one probe beam interact in a nonlinear medium to generate a signal beam that travels backward with respect to the probe beam and has a wave front that is conjugate to the probe beam. Similar to its application in solid-state laser amplifiers [7], DFWM in plasma may be used to compensate for wave-front distortion in plasma-based high-intensity laser amplifiers.

DFWM based on plasma gratings driven by the laser ponderomotive force was first analyzed by Steel and Lam [8] and the effect of thermal force was later included in the analysis by Federici and Mansfield [9], which shows that thermal force can greatly enhance the reflectivity (the ratio of signal beam intensity to probe beam intensity). Domier and Luhmann [10] analyzed nearly degenerate four-wave mixing, in which the two pump waves have the same frequency and the signal wave has a frequency slightly different from that of the pump waves. In this condition, the reflectivity is greatly enhanced if the frequency difference is equal to the frequency of the ion-acoustic mode of the plasma, which is referred to as Brillouin-enhanced, or resonant, four-wave mixing [10,11]. Experimental investigation of DFWM in plasma was first reported by Kitagawa *et al.* [12]. The experiment was done in the far-infrared regime with a long pulse. The observed n^6 dependence of the reflectivity on plasma density n showed that the grating formation was dominated by the thermal force instead of the ponderomotive force. Nearly degenerate four-wave mixing has also been demonstrated by Domier and Luhmann [10]. The experiment was done in the microwave regime and enhancement by the ion-acoustic wave was observed. A review of both degenerate and resonant four-wave mixing was given by Joshi *et al.* [13].

Concerning the dependence on wavelength λ, theoretical analyses [8,9,12,14] show that the reflectivity of DFWM is proportional to λ^6 when the formation of the plasma grating is dominated by the laser ponderomotive force, and it is proportional to λ^{10} when the formation of the plasma grating is dominated by the thermal force. Therefore, it is expected that a much higher laser intensity is required to achieve DFWM in the near-infrared regime, where chirped-pulse-amplification lasers are available, than in the far-infrared or microwave regime. In this paper, we report the demonstration of degenerate four-wave mixing in the near-infrared regime. The four-wave mixing process is verified by null tests and the dependence of the reflectivity on the temporal overlap of the laser pulses. The reflectivity is found to be proportional to the pump intensity and is independent of probe intensity in accordance with theoretical analyses. The quadratic dependence of the reflectivity on plasma density verifies that under our experimental conditions the quasineutral plasma grating is predominantly driven by the laser ponderomotive force rather than the thermal force.

II. PRINCIPLES AND ANALYSIS

The third-order susceptibility of a plasma for DFWM was first derived by Steel and Lam [8] and later generalized by Federici and Mansfield [9] as

$$\chi^{(3)} \cong \frac{n_0/{n_c}^2}{8(4\pi)^2(T_e+T_i)}\left(1+\sum_{i=f,b}\frac{n_0\nu_e}{(\mathbf{k}_i-\mathbf{k}_p)^2\kappa_e}\right), \qquad (1)$$

where n_0 is the plasma density, n_c is the critical density, T_e and T_i are the electron and ion temperatures in energy units,

ν_e is the electron-ion collision frequency, κ_e is the electron thermal conductivity, and $\mathbf{k}_i$ and $\mathbf{k}_p$ are the laser wave vectors. The reflectivity is given by

$$R = \frac{I_s}{I_p} \cong \kappa^2 L^2, \tag{2}$$

where

$$\kappa \cong \left| \frac{2\pi\omega}{c} \chi^{(3)} \cdot \mathbf{E}_f \mathbf{E}_b \right|, \tag{3}$$

in which $\mathbf{E}_f$ and $\mathbf{E}_b$ are the fields of the forward and backward pump pulses, respectively, the center dot denotes the tensor product, and L is the interaction length [5].

The process of DFWM can be understood from the nonlinear susceptibility $p^{(3)}=\chi^{(3)}E_fE_bE_p$. Let

$$E_f = \frac{A_f}{2}(e^{i\theta_f} + e^{-i\theta_f}),$$

$$E_b = \frac{A_b}{2}(e^{i\theta_b} + e^{-i\theta_b}),$$

$$E_p = \frac{A_p}{2}(e^{i\theta_p} + e^{-i\theta_p}), \tag{4}$$

where

$$\theta_f = \mathbf{k}_1 \cdot \mathbf{r} - \omega t + \phi_f,$$

$$\theta_b = -\mathbf{k}_1 \cdot \mathbf{r} - \omega t - \phi_b,$$

$$\theta_p = \mathbf{k}_2 \cdot \mathbf{r} - \omega t + \phi_p. \tag{5}$$

It can be seen readily that $p^{(3)}$ can be written as

$$p^{(3)} = \chi^{(3)} \sum_i \frac{A_i}{2}(e^{i\theta_i} + e^{-i\theta_i}), \tag{6}$$

where θ_i are combinations of θ_f, θ_b, and θ_p, and A_i are the corresponding products of amplitudes. Among all these combinations, the only term that contains $-\mathbf{k}_2\cdot\mathbf{r}-\omega t$ is $\theta_c=\theta_f+\theta_b-\theta_p=-\mathbf{k}_2\cdot\mathbf{r}-\omega t-\phi_p+\phi_f-\phi_b$. For a fixed $\phi_f-\phi_b$, this term has a phase conjugate to E_p and propagates in the opposite direction. Therefore this is the phase-conjugate reflection.

The physical origin of the third-order nonlinear susceptibility is the two plasma gratings generated by the beat patterns of the pump beams and the probe beam [15]. With a small angle between the forward pump and the probe in our experiment, the beat pattern of the forward pump and the probe produces a long-wavelength grating and the beat pattern of the backward pump and the probe produces a short-wavelength grating. The short-wavelength grating reflects the forward pump into the direction opposite to the probe beam, and the long-wavelength grating does the same by reflecting the backward pump. In our experiment the two reflected waves have orthogonal polarizations; therefore the intensity of the reflected signal I_s can be written as the intensity sum of the two processes:

$$R = \frac{I_s}{I_p} = \frac{I_b R_{fp}}{I_p} + \frac{I_f R_{bp}}{I_p}, \tag{7}$$

where

$$R_{fp} = \left| \frac{2\pi\omega}{c} \chi^{(3)} \cdot \mathbf{E}_f \mathbf{E}_p \right|^2 L^2 \tag{8}$$

is the reflectivity of the grating produced by the forward pump and the probe and

$$R_{bp} = \left| \frac{2\pi\omega}{c} \chi^{(3)} \cdot \mathbf{E}_b \mathbf{E}_p \right|^2 L^2 \tag{9}$$

is the reflectivity of the grating produced by the backward pump and the probe. In the limit of small plasma grating amplitude and reflectivity, R_{fp} and R_{bp} are given by the Bragg scattering formula

$$R_{ip} = \left(\frac{\pi}{2} \frac{\Delta n_i}{n_c} \frac{L}{\lambda} \right)^2, \tag{10}$$

where $i=(f,b)$, λ is the laser wavelength, and Δn_i is the density modulation. By comparing Eqs. (8)–(10), the amplitude of the plasma density grating $\Delta n_i/n_0$ can be written as [12]

$$\frac{\Delta n_i}{n_0} = \frac{1}{4} a_i a_p \frac{mc^2}{T_e + T_i}(1 + A), \tag{11}$$

where $a_i=eE_i/m\omega c$ and $a_p=eE_p/m\omega c$ are the normalized vector potentials of the laser beams and m is the electron mass. The first term is the contribution from the ponderomotive force, and the second term, $A=n_0\nu_e/(\mathbf{k}_i-\mathbf{k}_p)^2\kappa_e$, is the contribution from the thermal force that originates from inhomogeneous distribution of inverse bremsstrahlung heating. Substituting Eq. (10) into Eq. (7), the reflectivity R of the probe scales as

$$R \propto n_0^2 I_f I_b L^2 \lambda^6 \tag{12}$$

when the ponderomotive force is dominant, and scales as

$$R \propto n_0^6 I_f I_b L^2 \lambda^{10} \tag{13}$$

when the thermal force is dominant.

For a pump intensity of 7.3×10^{15} W/cm^2, a probe intensity of 3.0×10^{15} W/cm^2, a plasma density of 3.5×10^{19} cm^{-3}, a pulse duration of 500 fs, and a laser wavelength of 810 nm, A is on the order of 1×10^{-6}. Therefore the formation of the plasma grating and thus the probe reflectivity should be dominated by the ponderomotive force instead of the thermal force under such conditions. Note that all the above analyses are based on the assumption of a quasineutral plasma grating, which is applicable for long pulse duration. In the early stage of the interaction the laser beat pattern drives an electron grating, while the ions are uniformly distributed. Afterward, the Coulomb force drags ions to form a quasineutral plasma grating in which the density modulation depth increases greatly. The time for reaching quasineutrality can be estimated from the time for the ions to move a distance of half a wavelength of the plasma density grating, i.e., $\delta t_{ion}=\sqrt{M\pi/(mc^2k^2a_pa_b)}$, where M and

m are the ion and electron mass, respectively. The time scale is about 350 fs for a hydrogen plasma grating of 400-nm wavelength. With a laser pulse duration of 500 fs it is expected that such a plasma grating should reach quasineutrality within the pulse duration. Under these conditions the amplitude of the plasma grating, i.e., the density modulation depth, is determined by the balance between the laser ponderomotive force and electron thermal pressure.

With the probe beam incident at a small angle with respect to the forward pump, the wavelength of the plasma grating driven by the backward pump and the probe is much smaller than that driven by the forward pump and the probe. Because the short-wavelength grating should have a larger amplitude of density modulation due to the much shorter time needed for reaching quasineutrality, it is expected that in such a ponderomotive-force-dominated regime the contribution to the probe reflectivity from the short-wavelength grating should be much larger than that from the long-wavelength grating, the opposite of what occurs in a thermal-force-dominated regime [12].

III. SETUP

A 10-TW, 45-fs, 810-nm, and 10-Hz Ti:sapphire laser system with a bandwidth of 20 nm based on chirped-pulse amplification is used in this experiment (upgraded from the laser system in Ref. [16]). The setup is shown in Fig. 1. Both the forward and backward pumps are filtered by a 2.0-cm hard aperture and then focused respectively by a 30-cm-focal-length off-axis parabolic (OAP) mirror onto the gas jet. The focal spots are both 13 μm in diameter in full width at half maximum (FWHM) with 90% of the energy enclosed in a Gaussian-fit profile. The peak intensity is 7.3×10^{15} W/cm^2 for 8.1-mJ pulse energy and 500-fs duration. The probe pulse with a clear aperture of 4 cm is incident with an angle of 20° with respect to the forward pump and focused by a 30-cm-focal-length OAP mirror onto the same gas jet. The focal spot is 8 μm FWHM with 80% of the energy enclosed in a Gaussian-fit profile. The peak intensity is 3.0×10^{15} W/cm^2 for 1.4-mJ pulse energy and 500-fs duration. The pulse duration of the three laser pulses was tunable by changing the grating separation in the pulse compressor. The hydrogen gas jet is produced by a pulsed valve with a supersonic conical nozzle. The density profile has a flattop region of 1 mm in length and a sharp boundary of 250 μm at both edges. The atom density is 3.5×10^{19} cm^{-3} at 700-psi (4.8×10^6 Pa) backing pressure. To prevent the colliding laser beams from propagating back to the laser system and thus causing damage in optical components, the three laser beams are all set to be circularly polarized with the field directions shown in Fig. 1(b). The quarter-wave plates are oriented to turn the backward pump into right-handed circular polarization and the forward pump into left-handed circular polarization, so both the *s*-polarized pump pulses are changed to *p* polarization after passing through the two quarter-wave plates and then dumped by the thin-film polarizers.

An additional advantage of such a polarization configuration is that the reflectivity contributed from the short- and long-wavelength gratings can be measured separately at the same time. To produce laser beat patterns the polarization of the probe is changed by a quarter-wave plate into left-handed circular polarization. As shown in Fig. 1(b), this quarter-wave plate also turns the reflection of the forward pump from the short-wavelength grating into *s* polarization and the reflection of the backward pump from the long-wavelength grating into *p* polarization. Thus the contributions from the two gratings are separated by the thin-film polarizer. The reflected backward pump is transmitted through the thin-film polarizer and is then measured by an imaging system. The reflected forward pump is reflected by the thin-film polarizer and is then measured by another imaging system through a 40-60 beam splitter. Each of the two imaging systems consists of a 16-bit charge-coupled-device camera, a camera lens, and a bandpass filter. The absolute reflectivity contributed from the two plasma gratings is calibrated by inserting a high-reflection mirror before the OAP mirror to reflect the probe beam back to each of the two imaging systems by setting the angle of the quarter-wave plate as 45° and 0°, respectively. The measured reflectivity is defined as the ratio of the integrated intensity in the signal image to that mea-

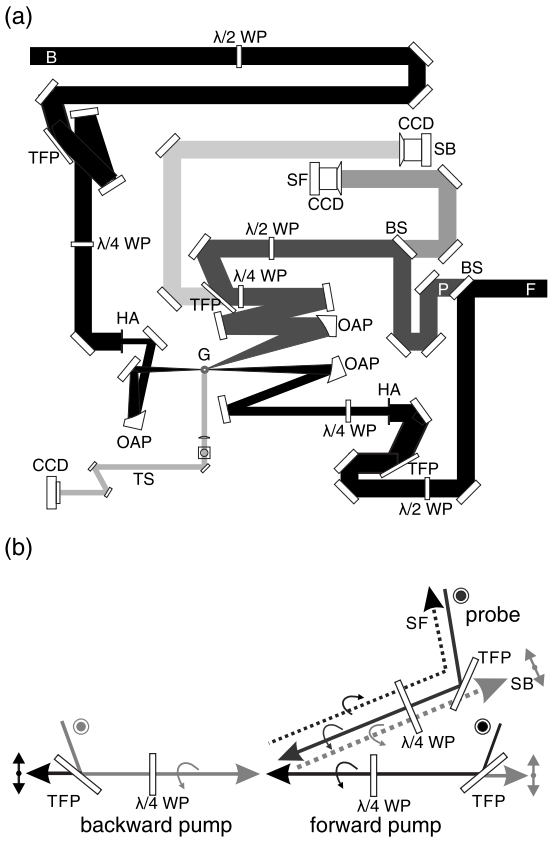

FIG. 1. Experimental layout (for clarity, the wall of the vacuum chamber is not shown) (a), and polarization configuration of the four laser beams (b). F, forward pump; B, backward pump; P, probe; G, gas jet; OAP, off-axis parabolic mirror; SF, imaging system that measures the reflected forward pump; SB, imaging system that measures the reflected backward pump; TS, imaging system for Thomson scattering; TFP, thin-film polarizer; BS, beam splitter; λ/4 WP, quarter-wave plate; λ/2 WP, half-wave plate; HA, hard aperture; CCD, charge-coupled-device camera.

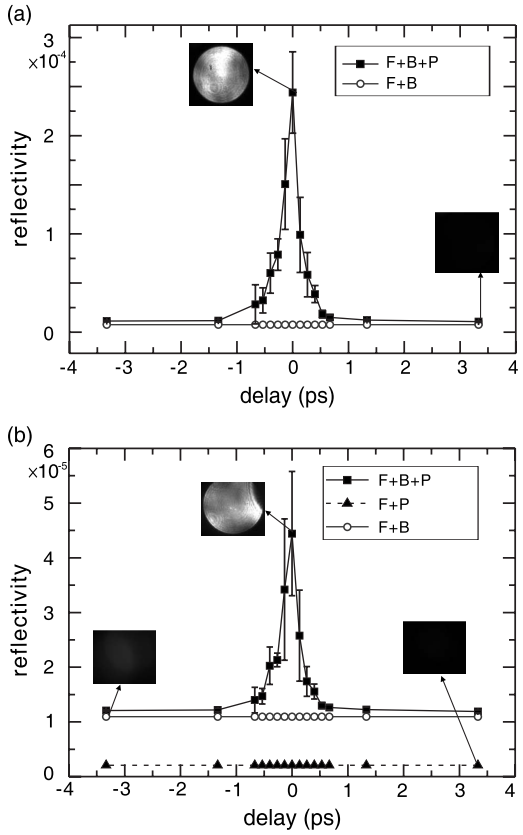

FIG. 2. Probe reflectivity contributed from the short-wavelength grating (a) and the long-wavelength grating (b), respectively, as a function of the delay of the probe pulse with respect to the pumps for various combinations of interacting laser beams. F, B, and P denote the forward pump, the backward pump, and the probe, respectively. The intensities of the forward and backward pumps are both 7.3×10^{15} W/cm^2, the intensity of the probe is 3.0×10^{15} W/cm^2, the plasma density is 3.5×10^{19} cm^{-3}, and the pulse durations for the three incident laser beams are all 500 fs.

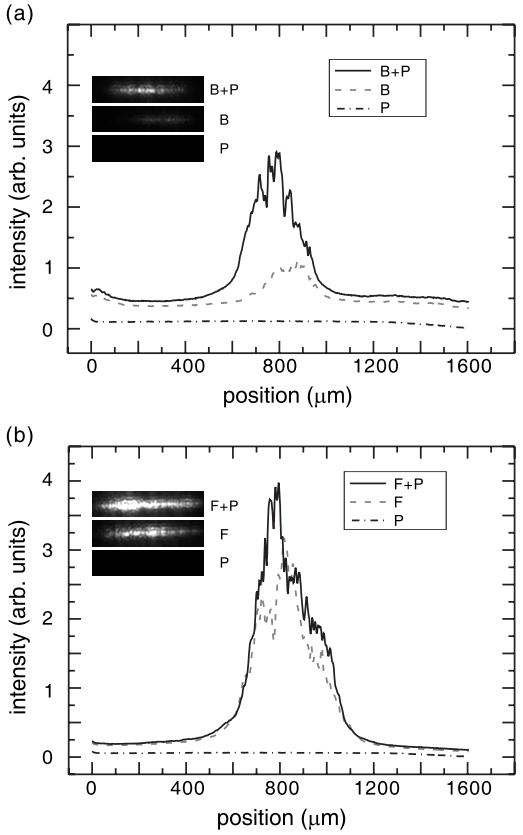

FIG. 3. Images and lineouts of Thomson scattering from each of the incident laser beams and their combinations. F, B, and P denote the forward pump, the backward pump, and the probe, respectively. The intensities of the forward and backward pumps are both 8.8×10^{17} W/cm^2, the intensity of the probe is 5.9×10^{16} W/cm^2, the plasma density is 3.5×10^{19} cm^{-3}, and the pulse durations for the three incident laser beams are all 45 fs. The focal spot sizes are all 8 μm in FWHM.

sured with the high-reflection mirror inserted. In addition, side imaging of Thomson scattering of the laser beams from plasma electrons is implemented to observe the formation of plasma gratings.

IV. EXPERIMENTAL RESULTS

Figure 2 shows the dependence of the probe reflectivities contributed from the short- and the long-wavelength gratings respectively, on the delay of the probe pulse with respect to the pumps. The intensities of the forward and backward pumps are both 7.3×10^{15} W/cm^2, the intensity of the probe is 3.0×10^{15} W/cm^2, the plasma density is 3.5×10^{19} cm^{-3}, and the pulse durations for the three incident laser beams are all 500 fs. The signal beam disappears when any of the three incident laser beams is blocked. In addition, the signal beam appears only when the probe pulse overlaps with the two pump pulses in time, and the width of the reflectivity curve is about 500 fs in FWHM, which is about equal to the pulse duration of the three incident laser beams. These observations identify that the observed signal beam is produced via a four-wave mixing process. The reflectivity contributed from the short-wavelength grating is about an order of magnitude larger than that from the long-wavelength grating, which is consistent with the theoretical expectation. In the data for reflection from the long-wavelength grating, significant background is observed whenever the backward pump is turned on. The origin of this background is that a small portion of the backward pump is collected by the OAP mirror of the probe beam even when no plasma grating is present, since the OAP mirror is at a small angle with respect to the opposite direction of propagation of the backward pump.

The presence of the plasma gratings that mediate the four-wave mixing process can be detected via Thomson scattering. Figure 3 shows the images and lineouts of Thomson scattering from each of the incident laser beams and their combinations. The intensities of the forward and backward pumps are both 8.8×10^{17} W/cm^2, the intensity of the probe is 5.9×10^{16} W/cm^2, the plasma density is 3.5×10^{19} cm^{-3}, and the pulse durations for the three incident laser beams are all 45 fs. Because of the small cross section of Thomson scattering, the hard apertures of the two pump beams are removed in this measurement to increase the intensity of the pump beams. Without the hard aperture, the focal spot is

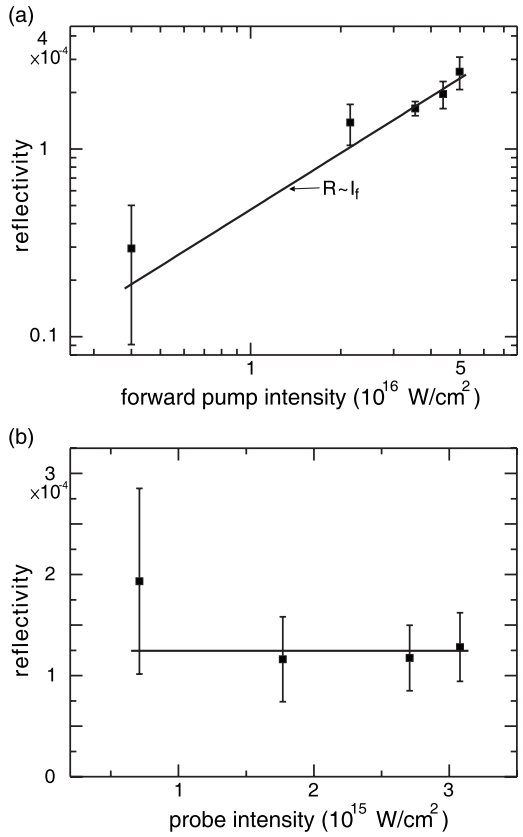

FIG. 4. Probe reflectivity contributed from the short-wavelength grating as a function of forward pump intensity at 3.0×10^{15} W/cm^2 probe intensity (a) and as a function of probe intensity at 7.3×10^{15} W/cm^2 forward pump intensity, (b). The intensity of the backward pump is 7.3×10^{15} W/cm^2, the plasma density is 3.5×10^{19} cm^{-3}, and the pulse durations for the three incident laser beams are all 500 fs. Solid lines are guides to the eye.

smaller, and more energy is passed through, at the expense of a shorter interaction length (Rayleigh range). The enhancement of Thomson scattering in the case with both the backward pump and the probe in comparison to the case with only the backward pump or the probe reveals the presence of the short-wavelength plasma grating, because the bunching of electrons with a scale length smaller than the laser wavelength can lead to coherent enhancement of Thomson scattering through constructive interference [17]. In contrast, only a slight enhancement in the Thomson scattering from the long-wavelength grating driven by the forward pump and the probe is observed, because the wavelength of the plasma grating is much larger than the laser wavelength.

Figure 4 shows the probe reflectivity contributed from the short-wavelength grating as a function of forward pump intensity at a probe intensity of 3.0×10^{15} W/cm^2 and as a function of probe intensity at a forward pump intensity of 7.3×10^{15} W/cm^2. The intensity of the backward pump is 7.3×10^{15} W/cm^2, the plasma density is 3.5×10^{19} cm^{-3}, and the pulse durations for the three incident laser beams are all 500 fs. The reflectivity shows a linear dependence on forward pump intensity and no dependence on probe intensity, both of which observations are consistent with the DFWM process.

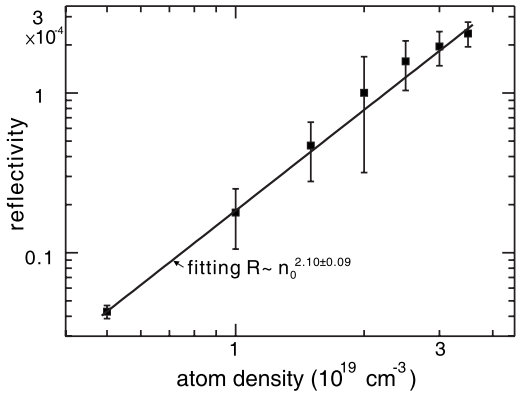

FIG. 5. Probe reflectivity contributed from the short-wavelength grating as a function of plasma density. The intensities of the forward and backward pumps are 7.3×10^{15} W/cm^2, the intensity of the probe is 3.0×10^{15} W/cm^2, and the pulse durations for the three incident laser beams are all 500 fs.

Figure 5 shows the probe reflectivity contributed from the short-wavelength grating as a function of plasma density. The intensities of the forward and backward pumps are 7.3×10^{15} W/cm^2, the intensity of the probe is 3.0×10^{15} W/cm^2, and the pulse durations for the three incident laser beams are all 500 fs. The reflectivity shows a quadratic dependence on plasma density. It confirms that under these experimental conditions the short-wavelength plasma grating is essentially quasineutral and the driving force is dominated by the laser ponderomotive force instead of the thermal force.

Figure 6 shows the probe reflectivity contributed from the short-wavelength grating as a function of pulse duration of the three incident laser beams. The energies of the forward and backward pumps are both 8.1 mJ, the energy of the probe is 1.4 mJ, and the plasma density is 3.5×10^{19} cm^{-3}. The optimal pulse duration is found at 500 fs for maximum reflectivity. Below the optimal pulse duration the reflectivity increases with increasing pulse duration. This can be ascribed to the increased plasma grating amplitude due to the

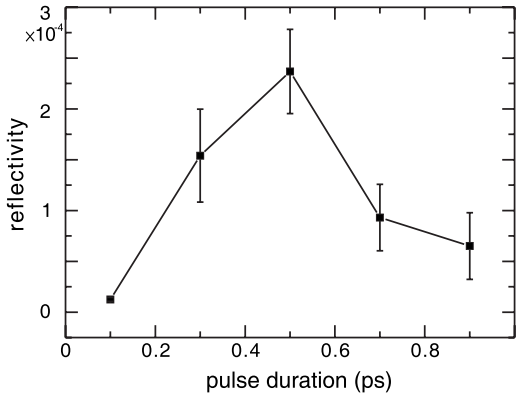

FIG. 6. Probe reflectivity contributed from the short-wavelength grating as a function of pulse duration of the three incident laser beams. The energies of the forward and backward pumps are both 8.1 mJ, the energy of the probe is 1.4 mJ, and the plasma density is 3.5×10^{19} cm^{-3}.

longer time for ion movement despite the decrease in the pump intensities. When the pulse duration is increased beyond the optimum, quasineutrality is well established, and the decrease in laser intensity with increasing pulse duration reduces the reflectivity.

As a result of the frequency chirp in the stretched laser pulses used in this experiment, the effective grating length is much shorter than the region of spatial and temporal overlap. If the two beating laser pulses are of significantly different frequency, the driven electron grating moves rapidly and thus the ions cannot follow the movement quickly enough to reach quasi-charge-neutrality. For two counterpropagating highly chirped pulses, only at the center of the interaction region the two pulses beat with the same instantaneous frequency throughout the pulse duration. Therefore only in that region can a quasistatic plasma grating be produced. If the motion of the ions lags behind that of the laser beat pattern by more than half a wavelength within the laser pulse duration, a grating cannot be produced effectively. This gives an effective plasma grating length of approximately $L_{\mathrm{eff}}=(\lambda_g/2)(1+\tau/\delta t_{ion})/(\delta\omega/\omega_0)$, where λ_g is the wavelength of the plasma grating, τ is the laser pulse duration, $\delta\omega$ is the bandwidth of the laser pulses, and ω_0 is the laser central frequency. This results in $L_{\mathrm{eff}}=20$ μm for the short-wavelength grating produced by 500-fs laser pulses. The maximum reflectivity measured in this experiment is 2.6×10^{-4}. Calculated using Eq. (10) and the 20-μm effective length, the amplitude of the short-wavelength plasma grating $\Delta n/n_0$ is about 1×10^{-2}. The amplitude of the plasma grating produced by laser beating in the near-infrared regime (1.054 μm) has been measured previously [17]. The experiment was done with a pulse duration, an interaction length, and a plasma density similar to ours. The laser intensities were 300 times higher than ours, and $\Delta n/n_0\approx10$ was measured. This agrees with the linear laser intensity dependence for each pump beam in Eq. (12).

V. CONCLUSION

In summary, near-infrared-regime degenerate four-wave mixing in a plasma has been demonstrated. The null tests and delay dependence identify the observed signal as the product of degenerate four-wave mixing. The presence of the mediating plasma grating is supported by the observation of enhancement in Thomson scattering of the laser beams. The dependence of the reflectivity contributed from the short-wavelength grating on both the forward pump intensity and the probe intensity agrees with the theoretical prediction. In contrast to the previous results obtained with long-wavelength lasers, the quadratic dependence on plasma density verifies that the DFWM is dominated by a quasineutral plasma grating driven by a ponderomotive force instead of a thermal force. The four-wave mixing process can be a useful tool for the diagnosis of plasma temperature and magnetic field [14], and phase-conjugate mirrors based on degenerate four-wave mixing in a plasma in the near-infrared regime may find important applications in eliminating nonlinear propagation effects in ultrahigh-intensity optics.

ACKNOWLEDGMENT

This work was supported by the National Science Council of Taiwan under Contract No. NSC 95-2112-M-001-005.

[1] D. Strickland and G. Mourou, Opt. Commun. **56**, 219 (1985).
[2] G. Shvets, N. J. Fisch, A. Pukhov, and J. Meyer-ter-Vehn, Phys. Rev. Lett. **81**, 4879 (1998).
[3] V. M. Malkin, G. Shvets, and N. J. Fisch, Phys. Rev. Lett. **82**, 4448 (1999).
[4] R. W. Hellwarth, J. Opt. Soc. Am. **67**, 1 (1977).
[5] A. Yariv and D. Pepper, Opt. Lett. **1**, 16 (1977).
[6] D. M. Bloom and G. C. Bjorklund, Appl. Phys. Lett. **31**, 592 (1977).
[7] G. S. He, Prog. Quantum Electron. **26**, 131 (2002).
[8] D. G. Steel and J. F. Lam, Opt. Lett. **4**, 363 (1979).
[9] J. F. Federici and D. K. Mansfield, J. Opt. Soc. Am. B **3**, 1588 (1986).
[10] C. W. Domier and N. C. Luhmann, Jr., Phys. Fluids B **5**, 2398 (1993).
[11] G. P. Gupta and B. K. Sinha, Phys. Plasmas **5**, 2252 (1998).
[12] Y. Kitagawa, R. L. Savage, Jr., and C. Joshi, Phys. Rev. Lett. **62**, 151 (1989).
[13] C. Joshi, Y. Kitagawa, and A. Lal, Int. J. Nonlinear Opt. Phys. **1**, 1 (1992).
[14] J. F. Federici, IEEE Trans. Plasma Sci. **19**, 549 (1991).
[15] Z.-M. Sheng, J. Zhang, and D. Umstadter, Appl. Phys. B: Lasers Opt. **77**, 673 (2003).
[16] H.-H. Chu *et al.*, Appl. Phys. B: Lasers Opt. **79**, 193 (2004).
[17] P. Zhang *et al.*, Phys. Plasmas **10**, 2093 (2003).